

ISSN: 2523-5672 (Online)

Water Conservation & Management

(WCM) DOI: http://doi.org/10.26480/wcm.03.2025.583.594



CODEN: WCMABD

RESEARCH ARTICLE

STEADY-STATE GROUNDWATER FLOW MODELING TO ASSESS WATER DEMAND IN ERBIL CITY, NORTHERN IRAQ

Radhwan G. Alkassar a*, Yousif H. Al-Aqeeli $^{\rm a,b}$, Zeyad Sulaiman a

- ^aDams and Water Resources Engineering Department, College of Engineering, University of Mosul, Mosul, Iraq.
- ^bDams and Water Resources Research Center.
- *Corresponding Author Email: radhwan.22enp57@student.uomosul.edu.iq

This is an open access journal distributed under the Creative Commons Attribution License CC BY 4.0, which permits unrestricted use, distribution, and reproduction in any medium, provided the original work is properly cited

ABSTRACT

Article History:

Received 11 June 2025 Revised 21 July 2025 Accepted 17 August 2025 Available online 12 September 2025 A steady-state groundwater flow model was proposed to examine how rising water demand in Erbil City affects the groundwater level in Northern Iraq. In GMS 10.8.6, the model was developed and it was calibrated to 2007 data of groundwater levels for 13 wells by going through a trial-and-error optimization process. GMS used the Newton Solver package (NWT) to strengthen the accuracy and consistency of its groundwater flow calculations. Model quality was evaluated using statistical indicators (ME, MAE, RMSE, and NSE). The calibration performance reached 0.962 in 2007, while for the years 2010, 2013, 2016, 2019, 2022, and 2024 the values ranged between 0.809 and 0.966 during validation. The forecasts for the future were done for the years 2027, 2029, 2031, 2033 and 2035 by assuming different rates of groundwater abstraction (20% for 2027 and going up to 100% in 2035) and groundwater recharge used the monthly average rainfall values from 1991 to 2022. Groundwater dropped citywide as demand for water increased. Groundwater head trends, estimated using Mann-Kendall and Sen's slope, found every observation well displayed extreme downward trends (p = 0.027), suggesting a steady decrease in all the areas. The values of R² between what the model predicts and what happens in reality were from 0.827 to 0.972, showing that the model works very well. In ArcMap 10.8, the spatial interpolation shown consistent descent of groundwater levels across several urban areas. It is necessary to create planning for water resources now and in the future and to target interventions where big drops are noticed. With the model, we can estimate how groundwater responds to future urban water demand

KEYWORDS

Groundwater modeling, Steady-state flow, Water resource management.

1. Introduction

The drinking water, agricultural and industrial activities in Erbil depend a lot on groundwater (Qarani and Sabah, 2022). Rainfall in Erbil city is sufficient because the area receives a significant amount of rain each year which recharges the groundwater. In Erbil City, semi-arid regions, pressure on the groundwater in urban areas is increasing because of variations in climate, more people and faster urban developments (Khayyat et al., 2019). For the residents of Erbil, groundwater is the most important source of drinkable water, so its well-being is very important (Margat and Van der Gun, 2013). Recent decades have seen Erbil's population rise quickly due to better stability and job opportunities, putting more pressure on natural resources, especially the groundwater (Ismael and Aziz, 2024). For this reason, the demand for drinking water is very high (FAO, 2014; United Nations, 2022). Since Erbil has grown, more groundwater is being used which raises serious concerns about overusing and eventually exhausting the aquifer. For these areas, consistently watching and analyzing the state of groundwater is necessary to achieve sustainable management. Considering these issues, using analytical studies to study groundwater behavior and see changes in water levels is now required. Different researchers have begun vintage research towards studying changes in groundwater and using computer models to see how aquifers react to different influencing elements. Research pointed out the use of advanced modeling and GIS for understanding groundwater supplies and predicting outcomes of planned projects at regional levels (Zhou and Li, 2011). Merz, in 2012, explained guidelines for groundwater and contaminant modeling, saying it should be done with stakeholders, have a clear goal and involve improving the conceptual model (Merz, 2012). Modeling groundwater is very helpful for water resources planning, especially in evaluating how well aquifers respond to people's activities and guiding related engineering projects; it is important, however, to be selective and thoroughly check the abilities of the software used (Kumar, 2012). For areas with little rain, groundwater management is easier when simulated models are used, especially with help from remote sensing and GIS (Singh, 2014). As indicates, using optimization supported groundwater models in parameter estimation well and in guiding optimal and cost-saving decisions (Yeh, 2015). According to the article, computer modeling can be used in exploring aquifers' response to population and climate change and in helping manage groundwater (Panahi et al., 2018). As applied hydrogeological modeling in studies of abandoned mines and found that their water level varies seasonally and therefore they do contain water (Wang et al., 2020). Employed GMS to investigate groundwater in the Karvan Basin and found decreasing 30% of pumping as the best suggested action for sustainability (Bayat and others, 2020). As utilized GMS modeling to illustrate that the pollution from industry affected over 40% of the groundwater area, and its remediation was not easy, necessitating the use of numerical tools in groundwater protection (Zhao et al., 2021). MODFLOW modeling combined with remote sensing, revealed, showed low exploitation of groundwater in Western Iraq with potential for sustainable development through regional

Quick Response Code

Access this article online



Website: www.watconman.org DOI:

10.26480/wcm.03.2025.583.594

cooperation (Al-Muqdadi, 2012). In Mosul, high groundwater is causing severe infrastructure and health risks; a calibrated MODFLOW model was used to delineate areas of concern and assist with urban water management (Al-Taiee and Hasan, 2006). The groundwater level and the productivity of wells vary significantly in Tal Afar, with the maximum depth of 519 m and a yield of 37.28 L/sec; the GIS-based analysis indicated a northwest-southeast pattern of distribution (AlKnoo, 2022). Visual MODFLOW modeling showed Najaf's groundwater meets most of the demand, but climate change can increase aridity; therefore, the extraction must be restrained and monitoring increased (Kareem, 2018). Iraq MODFLOW modeling showed rainfall as the main origin of groundwater, and climate change affected most areas and surface runoff played a critical role in recharge (Al-Areedhi and Khayyun, 2019). Sabesian sub-basin groundwater flows northeast to southwest through two aquifers; modeling matched observed levels regulated by Lake Dukan (Ali and Salley, 2013). As spoke about groundwater quality in Kurdistan, Iraq, analyzing samples chemically and physically (Hawez et al., 2020). They found localized contamination but water is still suitable for human use after treatment. MODPATH, implemented in GMS, was used to model groundwater drawdown and contaminant flow in Qushtaba Plain with a view to emphasizing sustainable management (Seevan, 2020). Urban expansion in Erbil, as detected by remote sensing and GIS, led to a fast decline in groundwater and it is expected to continue (Faqe and Hashemi, 2015). A study indicated that drying groundwater levels in Erbil's semiarid regions are a result of too much use, drought and lack of sustainable management, meaning urgent action is needed to avoid even greater shortages (Nanekely et al., 2017). The examining of nitrate contamination trends in central Erbil, using GMS modeling, confirmed that there was a clear increase and the results agreed well with the real data (Yashooa and Mawlood, 2023). As constructed a groundwater flow model for Erbil's basins using GMS and rich data and optimized the model by PEST calibration and sensitivity analysis to support sustainable management (Mustafa and Mawlood, 2024; MODFLOW 2000).

To develop the understanding of groundwater flow in Erbil City, this study uses the Groundwater Modeling System (GMS) version 10.8.6 to create a

steady-state numerical model. With the help of complete hydrogeological data and calibration, the model examines what changes will happen in the aquifers during increased water usage from expanding towns and growing populations. Simulations were done to study expected groundwater level drops as far to 2035, keeping the recharge constant and raising the pumping rates in steps. The research reveals that water levels of groundwater are going down gradually, especially in places where there is a lot of pumping, pointing to how important it is to manage water properly. Modeling aquifer response in this way helps policymakers understand how the aquifers work and makes it possible for them to consider effective ways of securing Erbil's water supply in the long run.

2. MATERIALS AND METHODS

Most of the water required by the people, farms and small industries in Erbil City comes from groundwater (Jwan et al., 2021). It is necessary to look at groundwater patterns to achieve sustainable management and learn the effects of both human and environmental changes on the aquifer systems. It describes the framework used to model steady-state groundwater flow in Erbil City by means of GMS 10.8.6. Using this strategy,

hydrogeological features are described, data gathering is done, models are

built, simulations are done and predictions are made. The goal is to check how the aquifer responds to rising water needs and support ongoing sustainable management of groundwater. Following subsections cover the study area, the data sources, the modeling methods and calibration steps that were involved in this study.

2.1 Study Area and Data collection

Erbil is a huge city in the Kurdistan Region of Iraq and a historic site that has been inhabited continuously since the 6th millennium BC. It is in northern Iraq, about $36.1911^\circ N$ in latitude and $44.0092^\circ E$ in longitude. Erbil, on an area of about $13,165~\rm km^2$, is found $360~\rm km$ north of Baghdad. In the region, the city is a central place for politics, business and culture. The important location of China has greatly affected how it has grown over the years.

The research gathered data from nearby monitoring wells and took notice of groundwater levels occurring between 2000 to 2024 and reported by the Directorate of Groundwater in Erbil. Inside the central basin of Erbil, we have groundwater wells, as part of the three main basins: Kapran (in the north), Nawand (Central Sub-Basin) and Bashtepa (in the south) which is outlined in Figure (1). The central sub-basin measures about 1,400 km² and features aquifers formed from alluvial sediments and the upper and lower Bakhtiari Formations (Hassan, 1998).

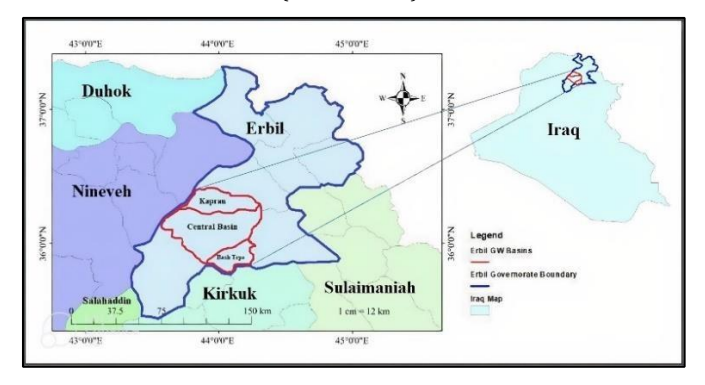


Figure 1: Map of study area (ArcMap 10.8)

The study analyzed data from 13 strategically located wells which recorded groundwater levels each month from 2000 to 2024 in Erbil City. Wells were chosen to include different locations and time frames of groundwater variation throughout the city. Table 1 shows the basic details and coordinates for the chosen monitoring wells used in developing the model.

The study analyzed data from 13 strategically located wells which recorded groundwater levels each month from 2000 to 2024 in Erbil City. Wells were chosen to include different locations and time frames of groundwater variation throughout the city. Table 1 shows the basic details and coordinates for the chosen monitoring wells used in developing the model.

Table 1: Location Coordinates of the Monitoring Wells								
Well Number	Monitoring Well Name	X (UTM)	Y (UTM)	Z Altitude (m)	Monitoring Period			
1	Badawa-12	414303	4002854	431	2006 - 2024			
2	Bahar New-4	408874	4002102	406	2006 - 2024			
3	Bagheshar Park	411158	4005256	415	2004 - 2024			
4	College of Science-1	411772	4001204	422	2004 - 2024			
5	Daratw Badel-18	412561	3998602	433	2001 - 2024			
6	Glkand Park	410708	4004622	405	2004 - 2024			
7	Grdarasha-3 Badel	411968	3995054	422	2002 - 2024			
8	Gulan Badel-8	415304	4006592	445	2006 - 2024			
9	Kasnazan-11	422212	4007342	627	2005 - 2024			
10	Nawroz Badel-13	407630	4003043	396	2004 - 2024			
11	Salahaddin-3	411210	4007388	395	2006 - 2024			
12	Shadi-26	406876	4001670	386	2006 - 2024			
13	Shorsh Badel-6	412026	4007318	426	2005 - 2024			

The locations of these wells cover districts including Zaniary, Nawroz, Shorsh, Khanaqa, Bahar, Shadi, Badawa, Sector 99, Kasnazan, Zheyan, Grdarasha, Daratw and Salahaddin and a map of these locations is shown in Figure (2).

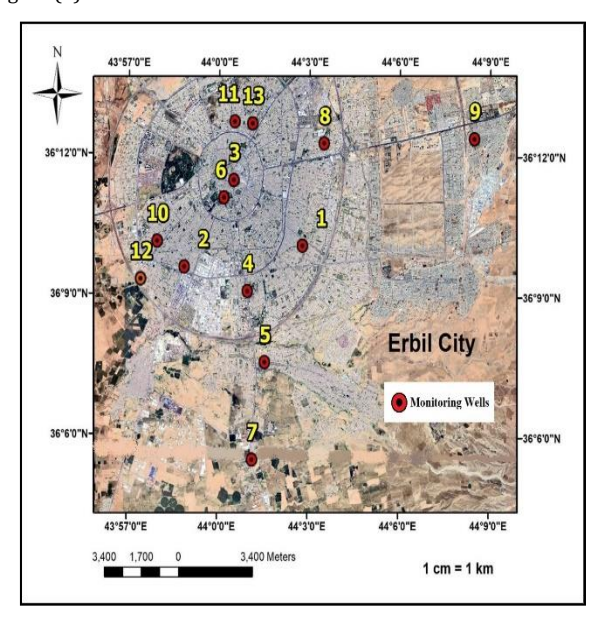


Figure 2: Erbil Satellite Map with Monitoring Wells Locations (ArcMap

The study area was delineated to cover $300~\rm km^2$ with dimensions of $15~\rm km \times 20~\rm km$, after accurately identifying the location of the central sub-basin and processing the Digital Elevation Model (DEM) using ArcMap $10.8.~\rm A$ rectangular boundary was purposefully chosen for several key reasons. It encompasses the entire urban area of Erbil City, includes all wells considered in the study (monitoring wells and public/private wells), and covers the core of the central sub-basin while remaining close to, yet not overlapping, the adjacent northern and southern sub-basins. As a result, there was less likelihood of interference from variations in rock types, porosity and ability of basins to store the fluid. The shape of the boundary helped design a grid system that made it much easier to set up the model in the GMS version $10.8.6.~\rm Figure$ (3) shows where the defined study area is located.

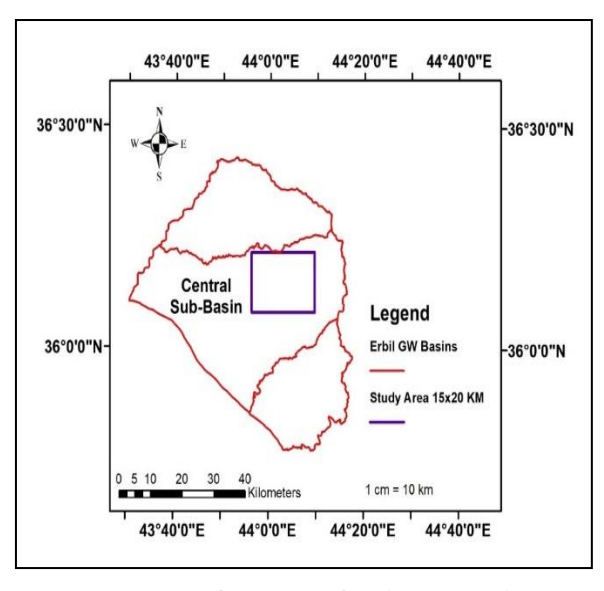


Figure 3: Study Area Boundary (ArcMap 10.8)

Besides the 13 wells analyzed here, there are 191 more wells found within the defined study area. These wells are mainly used for drinking water and are important for different purposes in Erbil City. There are 48 wells in the group that are set aside for private use and the remaining 143 wells provide water for the public and contribute to the potable water supply of the area. Information about these wells was provided by the Groundwater Directorate in Erbil, who supplied the locations and intended uses of the wells. These streams are crucial for ground water, helping the population cover its increasing demands for drinking, business and farming. Figure (4) displays where the wells are located within the study area, showing a general picture of the region's groundwater distribution.

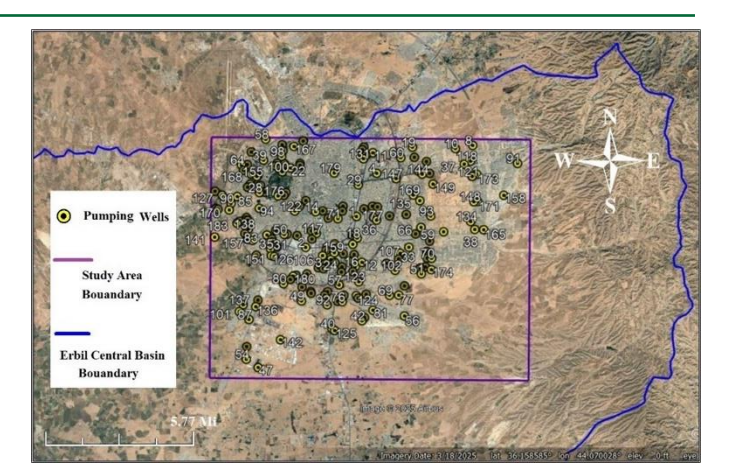


Figure 4: Satellite imagery showing the spatial distribution of public and private wells within the study area (Google Satellite View).

Additionally, information on rainfall in the Erbil region during the years 1991 to 2022 was obtained from the Erbil Meteorological Station. Data analysis led to groundwater recharge estimates and set the right boundaries for the model.

2.2 Groundwater Governing Equations

If the hydraulic head stays constant, that means at any given moment inflow and outflow are the same and the water storage does not change. This kind of model is favored for investigating where groundwater heads are in equilibrium. Only a single stress period and a single instant in time are required in steady-state simulations and all storage terms are made zero. In other words, to calculate the hydraulic head, just one equation is needed and it works regardless of how long the stress period or time step is (Fetter and Kreamer, 2021). Steady-state models were created in this study to predict groundwater levels in 2027, 2029, 2031, 2033 and 2035. For each model, the rate of pumping was set to be 20% higher in 2027 than in the base year 2024 and this increase was added to the pumping rate each year after. Although each scenario is a stable one, running the simulations one after another helps assess the lasting effect of more pumping on groundwater levels, by making the assumption that the aquifers have stabilized (Harbaugh, 2005).

The steady-state equation of groundwater flow for a heterogeneous and anisotropic medium is presented in Equation (1) (Anderson et al., 2015):

$$\frac{\partial}{\partial x} \Big(K x \frac{\partial h}{\partial x} \Big) + \frac{\partial}{\partial y} \Big(K y \frac{\partial h}{\partial y} \Big) + \frac{\partial}{\partial z} \Big(K z \frac{\partial h}{\partial z} \Big) = \, 0$$

Where:

K(x,y,z): Hydraulic conductivity in the directions (x,yz), with units of $(L T^{-1})$.

h: Hydraulic head, with units of (L).

 $\frac{\partial h}{\partial x}$: Partial derivative of h with respect to x.

 $\frac{\partial h}{\partial y}$: Partial derivative of h with respect to y.

 $\frac{\partial h}{\partial z}$: Partial derivative of h with respect to z.

These partial differential equations (PDEs) are commonly solved with numerical tools such as finite difference, finite element or boundary element methods to predict groundwater flow in different settings. The solutions to these equations let researchers understand groundwater flow, understand what aquifers are like and see the role of various factors on this system (Anderson et al., 2015).

2.3 Preparation and Modeling of Groundwater Flow Using GMS Software:

A conceptual model was put together to model groundwater flow that stays the same over time. The simulation was done by using the NWT Solver module from MODFLOW that uses finite-difference methods. The process breaks up the groundwater region with size $(\Delta x, \Delta y, \Delta z)$ into a grid of cells, replaces the flow equation derivatives with finer differences and then uses various numerical solutions to solve the set of equations considering boundaries and groundwater characteristics for every cell (Fetter and Kreamer, 2021).

MODFLOW includes the Newton Solver-NWT which solves groundwater flow problems in unconfined and semi-confined aquifers where the water table is not stable. The Newton-Raphson algorithm is applied by NWT to solve nonlinear equations, especially because it can simulate dry parts of unconfined aquifers (Akram and Ann, 2015). The approach involves going up winding to figure out horizontal hydraulic conductivity which guides the handling of drying and rewetting issues. For dry cells, the WEL package was improved to set their pumping rates to zero to make sure the system still converges. There are some adjustments to the SFR and UZF packages in MODFLOW-NWT to prevent moving water from dry cells and it still acts nearly like MODFLOW-2005 in simulations without dry cells or problems related to flow (Niswonger et al., 2011). An outline of the key steps for building a groundwater flow model is seen in Figure (5).

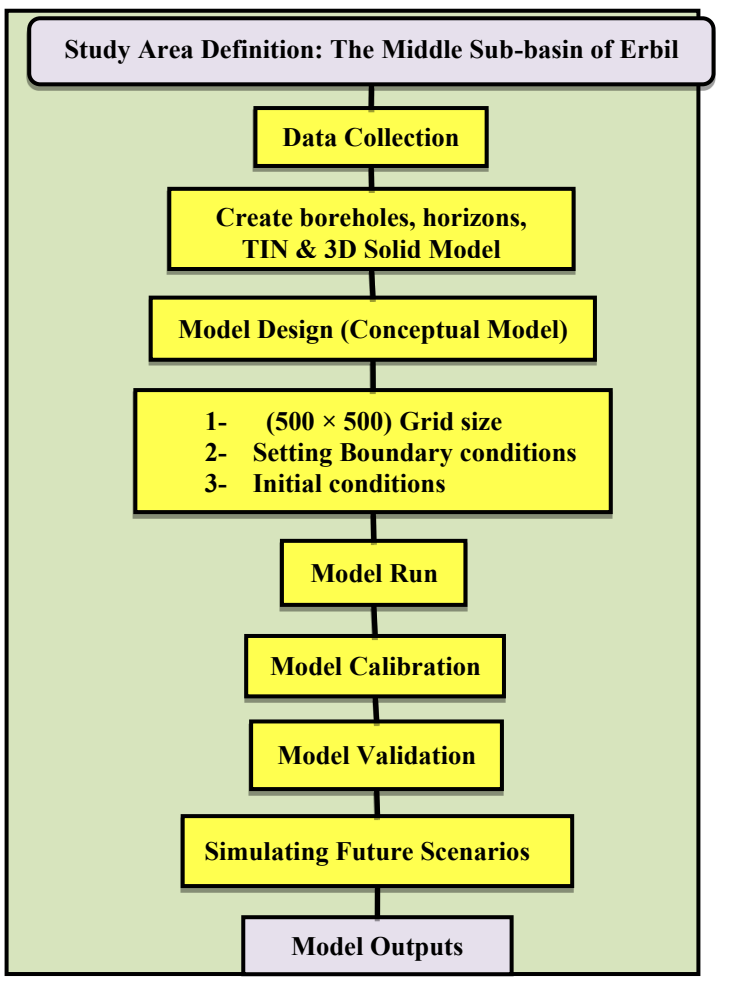


Figure 5: Flowchart of the study and GMS applications

2.3.1 Monitoring Wells Setup Using GMS Software

After designing the study area, GMS version 10.8.6 helped to add the monitoring wells into the model. The geometric information was based on WGS 1984, UTM Zone 38N to keep all data and maps from Google Earth, DEM files and ArcMap aligned. Using data from the Erbil Groundwater Directorate, 13 new monitoring wells were placed according to their coordinates, depths and lithology. The location and structure of the monitoring wells were added to the GMS model through the Borehole

Editor which also linked the geological layers in the model to the borehole data. Eventually, the wells were used to measure the model and ensure groundwater-level predictions in the model were accurate when checked with actual field measurements.

2.3.2 Linking Geological Layer Boundaries (Horizons)

The topography of the study area was built in GMS by creating a Triangulated Irregular Network (TIN) model. TIN triangles join elevation points, not in a grid but in a flowing irregular form which shows terrain features better than regular, square grids. The study area's elevation data from a 12.5-meter resolution Digital Elevation Model (DEM) was imported into GMS to create this network. The region for groundwater simulation was filled with a TIN mesh, using the built-in tools to make it compatible.

Both the monitoring wells and their subterranean layers (according to the boundaries set) were incorporated, after which the Auto Assign Horizons function in GMS was used to link aligned geological layers between the various wells. This tool allows to make surfaces that mark the dividing lines between different geological layers at every well site. The borehole images were processed to make surfaces at each horizon which showed where two neighboring geological layers touch. Every sedimentary layer was given a sequential number so that correlation and explanation would be the same everywhere. The process gave an accurate 3D image of the underground layers which was a foundation for creating a reliable model to simulate groundwater flow. Figure (6) reveals the well places in the model and draws the horizon lines to connect the layers, making sure that the same layer number is used for each discussed well.

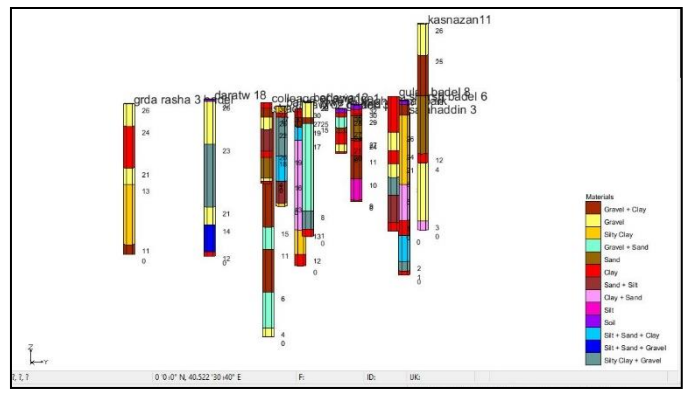


Figure 6: Side view of monitoring wells showing the assigned horizon numbers between geological layers (GMS 10.8.6)

2.3.3 Formation of the Solid Model

When the geological layers of the monitoring wells were connected using the horizon surfaces (Horizons), a solid model was built in GMS using the Horizons to Solid feature. It creates a unified 3D model showing the layers and structures found in the study area. Because the Digital Elevation Model (DEM) was integrated into the model, the virtual ground surface was displayed with accuracy. The simulation matches the real relief map which directly controls where and how groundwater moves. Having a solid model gives the scientific team superior grounds to design the simulation grid which closely represents the layered structure and elevation of the site. Figure (7) illustrates the formed solid model, where each different layer and its color is based on information from well data and their connection to the ground surface is clearly shown.

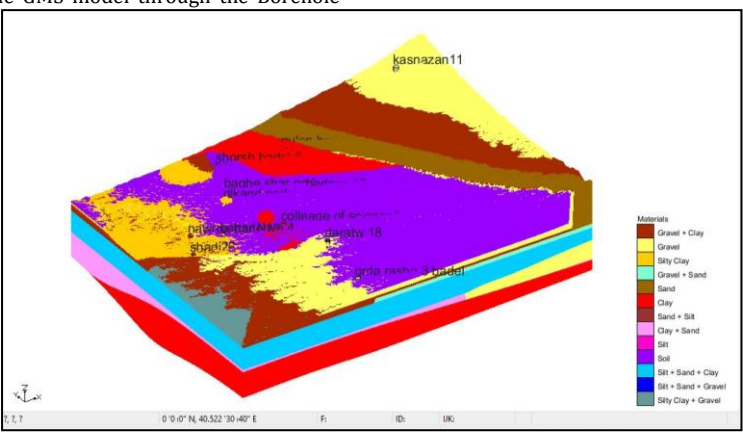


Figure 7: 3D Solid Model of the Study Area (GMS 10.8.6)

2.3.4 Converting the Grid Network to a 3D Solid Model

GMS was used to set up a three-dimensional grid inside a marked-out frame that covered the study area. The shape of the grid cells was chosen as $500~\text{m} \times 500~\text{m}$ so that both data accuracy and groundwater modeling were achieved. A grid consisting of 1,200 cells was formed on the domain by drawing 40 columns and 30 rows. Layer distribution was made vertically using 15 layers based on the information from wells and linked horizons, as explained before. Using this grid means that the simulation will be realistic and effective at the same time by representing hydrogeologic conditions inside the study borders.

A 3D Grid network was constructed and layers were defined and then

these were turned into a 3D Solid model using specific GMS tools to visually display the true structure of the geology in the study area. To do this, previously set horizons guided by depth data were depended on. Software process generated where volumetric solids should exist based on the grid cell's depth and length. Producing a 3D model allows one to link horizontal and vertical layer information which aids in simulating groundwater flow using MODFLOW. Detailed modeling of the flow and volume allows accurate property assignment as well as clear division of recharge and pumping sections and will support future testing scenarios. Figure (8) illustrates 3D Solid Model after converting the Grid network into volumetric cells.

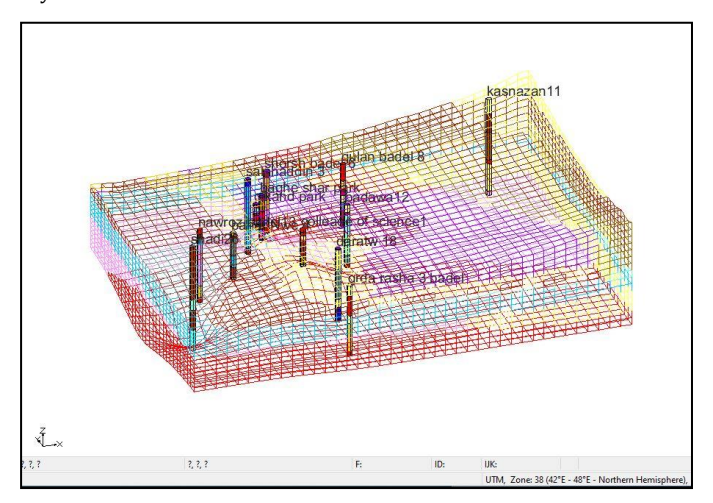


Figure 8: 3D Solid Model after converting the Grid network into

volumetric cells (GMS 10.8.6)

2.3.5 Initial Assignment of Hydraulic Properties to Geological Layers

The initial values for K were determined from the ranges reported in books by (Freeze and Cherry, 1979; Fetter and Kreamer, 2021). Following

the principles outlined in Table (2), the model was used to predict the hydraulic properties of the soil layers, where specific field measurements were not available on site.

Table 2: Ranges of Hydraulic Conductivity for Different Geological Formations (Freeze and Cherry, 1979)								
Type of Geological Formation	Minimum Hydraulic Conductivity (m/day)	Maximum Hydraulic Conductivity (m/day)						
Coarse gravel	864	8,640						
Sands and gravels	0.864	864						
Fine sands, silts	0.0000864	0.864						
Clay, shale, glacial	8.64E-09	0.0000864						
Dolomitic limestone	0.864	86.4						
Weathered chalk	0.864	86.4						
Limestone	0.0000864	0.0864						
Sandstone	0.00000864	8.64						
Granite, Gneiss, Compact basalt	8.64E-09	0.0000864						

Among the important hydraulic properties included in the model were horizontal and vertical conductivity (Kh and Kv), anisotropy ratio, specific yield, specific storage, porosity and longitudinal dispersion, using the data listed by (Fetter and Kreamer, 2021). Parameters were adjusted later to suit the local aquifer environment and the information in the modeled wells.

2.3.6 Model Setup Using MODFLOW-NWT in GMS

Simulating groundwater flow with steady conditions allowed the MODFLOW-NWT settings to show the long-term pattern of groundwater levels in the study area. Advanced options were added to the settings to better handle number stability and generate realistic results for the hydrological model. The input data needed for the MODFLOW-NWT model are presented in Table (3) and include the model domain, boundary conditions, recharge information, wells, aquifer conductivity and calibration method.

Table 3: Input data for the MODFLOW-NWT model setup in GMS					
Conceptual Model	Description				
Model Domain	Cell size (500 m × 500 m) with a thickness of 700 m				
Boundary Conditions	Constant hydraulic heads (CHD) were applied at monitoring well locations to represent boundary conditions over different time periods, aiming to calibrate hydraulic properties and compare results with observed data				

)RCH(Recharge Coverage	Recharge was calculated monthly using rainfall data, converting precipitation to recharge at a rate of 5% of the monthly values. Surface water areas within the model boundaries were included, with a recharge rate of 5.47282E-05
Observation Wells Coverage	A total of 13 wells within the study area were tested
Existing Wells Coverage	The number of production wells is 191
Hydraulic Conductivity (m\d)	According to the stratigraphic formation
Model Calibration	It was done by trial and error through gradual adjustment of parameters to achieve the best fit between calculated and observed data

Constant Head Boundaries (CHDs)

This package was used in a way that it was used to replicate steady-state hydraulic conditions at locations of 13 monitoring wells that were distributed in the study area. Starting and finishing groundwater heads were provided to the corresponding grid cells of these wells based on sporadic readings collected by the Erbil Groundwater Directorate for each of the monitoring wells.

Recharge (RCH)

The recharge amount entering the top layer was calculated using the RCH package from GMS, with precipitation (mm/day) acting as the input for the time span 1991–2022. These data were converted to monthly recharge rates (m/day) using the formula in Equation (12) (Fetter and Kreamer, 2021):

Recharge Flux (m\d) =
$$\left(\frac{\text{Rainfall (mm)}}{1000}\right) \times \frac{\text{Recharge Fraction}}{\text{Days of Month}}$$
 (2)

Where:

Recharge Flux: the recharge rate, in meters per day (m/day).

Rainfall (mm): the total monthly precipitation, in millimeters.

Recharge Fraction: the proportion of rainfall contributing to groundwater recharge.

Days of Month: the number of days in the month, used to calculate daily recharge.

The proposed 5% recharge rate was taken from, based on how much of the area is open land and how the water recharges (Lerner, 2002). After calculating the recharge amount, these values were assigned to the correct grid cells using soil permeability and topographic slope data in GMS to get a proper spatial representation. For modeled years, the annual average value for recharge was applied as a single figure to represent the actual water supply in those years.

Wells (WELs)

Pumping data from 191 public and private wells distributed throughout $\,$

the study area were also incorporated into the model. The figure considers all the wells up to the year 2024. A cumulative time model was constructed through adding wells incrementally per year according to their construction and operating start years. Each well was correctly located within the model, and its individual pumping rate assigned to the relevant hydrogeological layer.

2.3.7 Simulation Check and Model Run

Following the input of all data into the MODFLOW model inside GMS, a check was performed to verify that the model setup was correct and free of bugs. This included:

- Verifying alignment between geological layer boundaries, well locations, and hydrological boundary conditions (CHDs, RCHs, WELs).
- Ensuring that the first layer was fully covered with recharge values.
- Checking consistency between model simulation time and the periods of observed head data.
- Reviewing the active package settings and customized NWT options.

The Model Checker tool was used to find and fix issues and after this was done, the Run MODFLOW function was used to execute the model. The MODFLOW Run Dialog window reports iteration counts and error values and confirms that the simulation process has completed successfully.

2.3.8 Model Calibration

The calibration process for steady-state flow was done with data from 13 monitoring wells. There were reliable monthly measurements from every well in 2007, so that year was considered perfect for calibrating and validating the model. Adjusting hydraulic parameters such as hydraulic conductivity and specific storage/yield, involved a process of trial and error until they matched the observed water levels as close as possible. The parameters for the hydraulic model had to be adjusted according to changes in soil type within the study area. The following table (4) shows the adjusted parameter values for every soil type such as Kh, Kv, Ss, Sy and other key variables necessary for the model's accuracy.

	Table 4: Final Calibrated Parameter Values Used in the Model								
#	Soil Texture	Hydraulic Conductivity Aniso (m/d)		otropy	Specific Storage	Specific Yield (%)	Longitudinal Dispersion	Porosity (%)	
		Kh	Kv	Horiz.	Vert. (Kh/Kv)	(1/m)		Lx	
1	Gravel + Clay	398	149	1	2.67	2E-13	55.7	60.7	80.7
2	Gravel	9875	1680	1	5.88	7E-15	66.7	66.7	78.7
3	Silty Clay	153	32.7	1	4.68	8E-13	27.3	52.3	93.3
4	Gravel + Sand	7675	767.5	1	10	8E-15	61.7	62.7	72.7
5	Sand	6775	737.5	1	9.19	7E-14	74.7	72.7	80.7
6	Clay	0.143	0.0143	1	10	7E-16	5.17	6.07	78.8
7	Sand + Silt	353	176.5	1	2	8E-15	35.3	36.3	86.3
8	Clay + Sand	4.83	1.53	1	3.16	7E-14	25.8	28.8	90.3
9	Silt	323	29.7	1	10.88	8E-15	34.3	34.3	92.3
10	Soil	153	30.7	1	5	8E-14	27.3	28.8	86.3
11	Silt + Sand + Clay	48.7	9.74	1	5	8E-15	29.3	30.3	90.3

12	Silt + Sand + Gravel	397	198.5	1	2	7E-15	55.7	62.7	83.3
13	Silty Clay + Gravel	387	30.7	1	12.61	8E-13	30.3	32.3	88.3

In order to assess the calibration process, the Nash–Sutcliffe Efficiency (NSE) was applied (Equation 3; Nash and Sutcliffe, 1970). Interpretation of NSE values followed the performance criteria described by (Moriasi et al., 2007).

$$NSE = 1 - \frac{Sum \text{ of Squared Errors (SSE)}}{Total \text{ Sum of Squares (SST)}} = 1 - \frac{\sum_{i=1}^{n} (\text{Yobs-Ycomp})^{2}}{\sum_{i=1}^{n} (\text{Yobs-Mobs})^{2}}$$
(3)

Where:

NSE: Nash-Sutcliffe Efficiency coefficient.

n: Number of observation points.

SSE: Sum of squared errors between observed and computed values, calculated as: $\sum_{i=1}^n (Yobs-Ycomp)^2$

SST: Total sum of squares, calculated as: $\sum_{i=1}^{n} (Yobs - Mobs)^2$

Yobs: The observed value at the monitoring well.

Ycomp: The computed value by GMS at the monitoring well.

Mobs: Mean of observed values at monitoring wells.

The Nash-Sutcliffe Efficiency (NSE) ranges from - ∞ to 1. A value of 1 indicates a perfect match between the computed and observed values, while a value of 0 means the model's performance is equivalent to using the mean of the observed data. Negative NSE values indicate the model performs worse than simply using the observed mean. According to hydrological standards, NSE values above 0.65 are considered practically acceptable, values above 0.75 are good, and values above 0.85 are excellent. This metric is sensitive to outliers and may give an exaggerated evaluation if the data contain high variability.

In addition to the Nash-Sutcliffe Efficiency (NSE), the following statistical metrics were used to evaluate the model's performance during the calibration and validation phases:

Mean Error (ME): The Mean Error (ME) is calculated using Equation
(4). It reflects the bias (underestimation or overestimation) without
measuring the error magnitude (Montgomery et al., 2021):

$$ME = \frac{1}{n} \sum_{i=1}^{n} (Yobs - Ycomp)$$
 (4)

 Mean Absolute Error (MAE): This metric is more appropriate for assessing the error magnitude regardless of its direction (Willmott and Matsuura, 2005). MAE is calculated by Equation (5):

$$MAE = \frac{1}{n} \sum_{i=1}^{n} |Yobs - Ycomp|$$
 (5)

 Root Mean Square Error (RMSE): This metric is preferred when penalizing large errors (outliers) in evaluation, according to (Abraham and Ledolter, 2009). RMSE is calculated using Equation (6):

$$RMSE = \sqrt{\frac{1}{n} \sum_{i=1}^{n} (Yobs - Ycomp)^{2}}$$
 (6)

2.3.9 Model Validation

After calibration, the model was validated through analysis to see if it can properly describe groundwater flow under a variety of conditions throughout the years. Validation for the model used measurements from wells in the years 2010, 2013, 2016, 2019, 2022 and 2024 where groundwater levels were reliable. A model was built for every year, considering constant flow and the performance of each model was checked with the collected monthly data from those same years.

Each year, the data included numbers of pumping wells that existed up to that year, ensuring an accurate record of how groundwater use changed with time. The annual rainfall average was transformed into an effective recharge rate using Equation (2) for each year.

It was found that the groundwater head data from the model fitted the observations accuracy, with the Nash-Sutcliffe Efficiency (NSE) being 80.92% to 96.57%, indicating that the model represents groundwater behaviors well in the study area.

2.3.10 Groundwater Variation Prediction

Based on calibrations for 2024 which assembled 191 active production wells in the study area, several prediction models were run to evaluate the impact urbanization and rising populations could have on groundwater levels. To carry out the prediction, pumping rates from the wells were gently increased in line with scenarios that covered a forecast period running up to 2035. The tests were carried out at a steady state to see the system's response to different levels of stress.

The assumed scenarios included:

- A 20% increase in pumping by 2027.
- A 40% increase in pumping by 2029.
- A 60% increase in pumping by 2031.
- An 80% increase in pumping by 2033.
- A 100% increase in pumping by 2035.

A separate independent model was constructed for every year and the pumping rates were altered to show the required increase. To calculate recharge from rainfall, the average monthly rainfall between 1991 and 2022 was used and the result was expressed as meters per day. For every scenario, we kept the recurring monthly recharge the same which made it possible to compare actual results consistently and with accuracy. The purpose was to assess possible future changes in groundwater levels and to predict the expected amount of drawdown in various sections of the area. It was revealed that increasing pumping creates a slow drop in underground water levels, especially where there are many wells which points to the need for careful planning of future water supplies for sustainability.

2.4 Statistical Analysis Methodology of Predicted Water Levels

The Mann-Kendall Test and Sen's Slope Estimator methods were used on the prediction results from the numerical model for every observation well and for all forecast years to examine the trends and importance of changes in predicted groundwater levels. Analysis of the model's outputs was done to observe how the trends changed with new future pumping and recharge rates selected for the scenarios. Most of the analyzed wells showed a notable pattern, suggesting that the groundwater level is dropping slowly as water demand, the population and climate changes increase in the near future.

Mann-Kendall Test (MK)

A common way to recognize trends in hydrological and environmental time series is to use the Mann-Kendall test (MK). Its main strength is that it does not rely on each data point being normally distributed and it is unaffected by unexpected changes in series from different time periods. The test is usually employed to understand trends in rainfall and groundwater levels. It considers that the sample data are not connected one to another. The World Meteorological Organization suggests using this method to pick up and calculate changes in environmental data (Hassan, 1998) (K. Yenigu'n MSc, 2008). When conducting an MK test, the null hypothesis (H_0) assumes there is no significant direction and the alternative hypothesis (H_1) suggests there is a significant trend present. M is calculated as described in Equation (7) and its average is zero (Douglas et al., 2000) (K. Yenigün MSc, 2008).

$$M = \sum_{i=2}^{n} \sum_{j=1}^{i-1} sign (Ai - Aj)$$
 (7)

$$sign (Ai - Aj) = \begin{cases} 1, if (Ai - Aj) > 0, \\ 0, if (Ai - Aj) = 0, \\ -1, if (Ai - Aj) < 0. \end{cases}$$
 (8)

Where, M represents the Mann-Kendall statistic, which summarizes the direction of the trend, n is the time series length, Ai and Aj are the successive data values of the time series in the years i and j.

The test procedure begins by calculating the Mann-Kendall statistic value M using Equation (7) as described above, then its variance V(M) is calculated using the following Equation (9):

$$V(M) = \frac{1}{18} \left[n(n-1)(2n+5) - \sum_{p=1}^{q} tp(tp-1)(2tp+5) \right]$$
 (9)

Where, V represents the variance of the Mann-Kendall statistic (M), ti is the number of ties for pth value, and q is the number of tied values.

The standardized test statistic ZMK are computed as follows Eq. (10):

$$Z_{MK} = \begin{cases} \frac{M-1}{\sqrt{Var(M)}} & \text{if } M > 0, \\ 0 & \text{if } M = 0, \\ \frac{M+1}{\sqrt{Var(M)}} & \text{if } M < 0, \end{cases}$$
 (10)

If the ZMK value is positive, it refers to increasing trends, likewise the negative value of ZMK refers to decreasing trends in the time series (Douglas et al., 2000, K. Yenigu'n MSc, 2008). The null hypothesis is rejected when $|ZMK| > (Z1-\alpha/2)$. The critical value of standardized normal $(Z1-\alpha/2)$ can be obtained from the standardized normal table (Gordon, 2006); the value of $(Z1-\alpha/2)$ is 1.96 at the 5% significant level.

Sen's Slope Estimator

When a linear trend is present in a time series, the true slope (change per unit of time) can be estimated using a simple nonparametric method introduced by (Hirsch and Slack, 1984). It has been widely used for determining the magnitude of the trend in hydro-meteorological time series (Sen, 1968; Tabari et al., 2011; Tabari et al., 2015). In this method, the slope estimates (Se) for N pairs of data (where N represents the total number of data pairs) are first calculated using the following expression Eq. (11):

Se =
$$\frac{Ei - Ek}{j - k}$$
 for e = 1,2,3, ... N (12)

where, Ei and Ek are data values at time j and k (j>k) respectively. The median of these N values of Se is Sen's estimator of slope which is calculated as Eq. (12):

$$\alpha = \begin{cases} Se[(N+1(N/2))/2] & N \text{ is odd} \\ \frac{1}{2}(Se + Se(N+2)/2) & N \text{ is even,} \end{cases}$$
 (12)

If α is positive it implies an upward (that is increasing) positive trend in the time series data whereas if α is negative it represents downward (that is decreasing) positive trend in the time series data.

2.5 Methodology for Spatial Analysis of Predicted Groundwater Levels Using ArcMap 10.8

Equipotential lines were plotted on ArcMap 10.8 from the estimates of groundwater levels in the wells found in the study area for every predicted year. With groundwater simulation data imported and processed using the programs' mapping tools, it became possible to draw maps that visualize where the groundwater table rises and falls. Plotting equipotential lines lets you know which way groundwater flows and highlights areas with large or low hydraulic gradient which helps understand the effects of pumping, population numbers and climate on the aquifer. Use of these lines helps in understanding water movement and making informed choices for water resource management.

3. RESULTS AND DISCUSSION

3.1 Calibration Results

The model was able to correctly capture the hydrogeological activities of the study area in 2007 which shows a high level of performance during calibration. To fix the parameters, the modeler conducted many (over 6,000) calibration trials by trial and error, testing conductivity, storage coefficients, permeability and longitudinal dispersion. It took seven and a half months of hard manual work to calibrate the model by adjusting it repeatedly and doing both visual and numerical assessments of the results. In the end, specific parameter values were found that achieved the best agreement between the simulations and the environmental data, as shown in Table (4).

Results were considered acceptable since the Mean error (ME) was about

-1.2 meters, the Mean Absolute error (MAE) was 1.81 meters and the Root Mean Square error (RMSE) was 2.44 meters. The Nash-Sutcliffe Efficiency (NSE) of 96.17% signified that the model is accurate in reproducing continuously stable water level values. Praful stated that these indicators show how well the calibration went by demonstrating an accurate model of the hydrological system which helps get reliable results from the validation and prediction stages.

The comparison results between the observed and simulated groundwater levels demonstrate an excellent representation for each observation well. Figure (9) illustrates the closeness of the simulated values to the observed ones through the distribution of symbols assigned by the software for each well along the diagonal symmetry line.

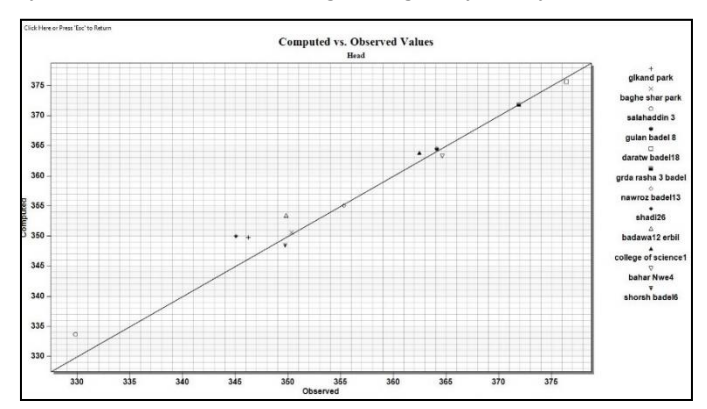


Figure 9: Relationship between simulated and observed groundwater levels along the diagonal symmetry line (GMS 10.8.6)

Figure (10) displays the observed and calculated groundwater levels during the model's calibration, revealing how the model fits the observed groundwater values.

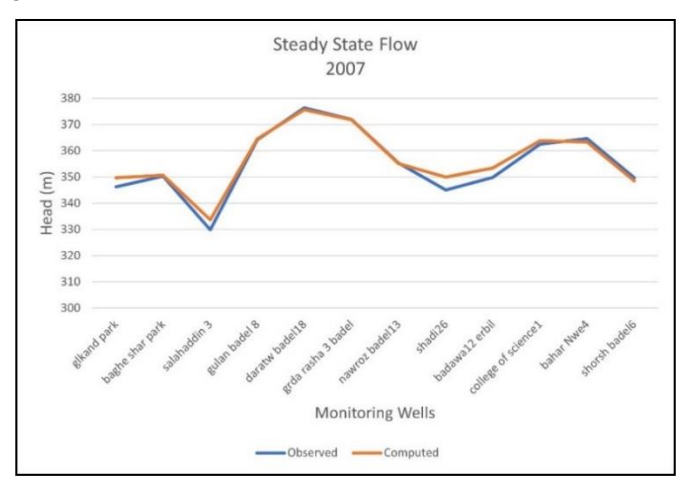


Figure 10: Graph showing the calibration results for the steady-state condition

3.2 Validation Results

Table (5) provides the results of how the simulation model works under steady-state flow conditions for all validation years. Each validation year contains the Nash-Sutcliffe Efficiency (NSE), Root Mean Squared Error (RMSE), Mean Absolute Error (MAE) and Mean Error (ME) as key indicators. Results from the model show that it is both precise and reliable in depicting groundwater levels and proves its strong ability to simulate the hydrogeology during those periods.

	Table 5: Performance Metrics of Simulation Models Using GMS 10.8.6							
#	Model Name	Validation Year	NSE	Mean Residual (ME)	Mean Absolute Residual (MAE)	Root Mean Squared Residual (RMSE)		
1	Validation - Steady State Flow	2010	92.14	-1.85	2.27	3.24		
2	Validation - Steady State Flow	2013	80.92	-4.94	5.39	6.29		
3	Validation - Steady State Flow	2016	91.79	-1.37	2.82	3.34		

4	Validation - Steady State Flow	2019	89.92	-3.36	4.69	7.32
5	Validation - Steady State Flow	2022	93.38	-3.49	3.97	5.64
6	Validation - Steady State Flow	2024	96.57	-1.42	3.13	4.46

3.3 Prediction Results

This section presents what is expected to happen to groundwater levels in thirteen monitoring wells during the given years: 2027, 2029, 2031, 2033 and 2035. The graphs (Figure 11) show the expected variations in water

levels for every well over these years which demonstrate the effect of higher pumping on the aquifer in the study region. Charts explain changes in groundwater trends over time and show what will happen to the same well's water table when there are different demands.

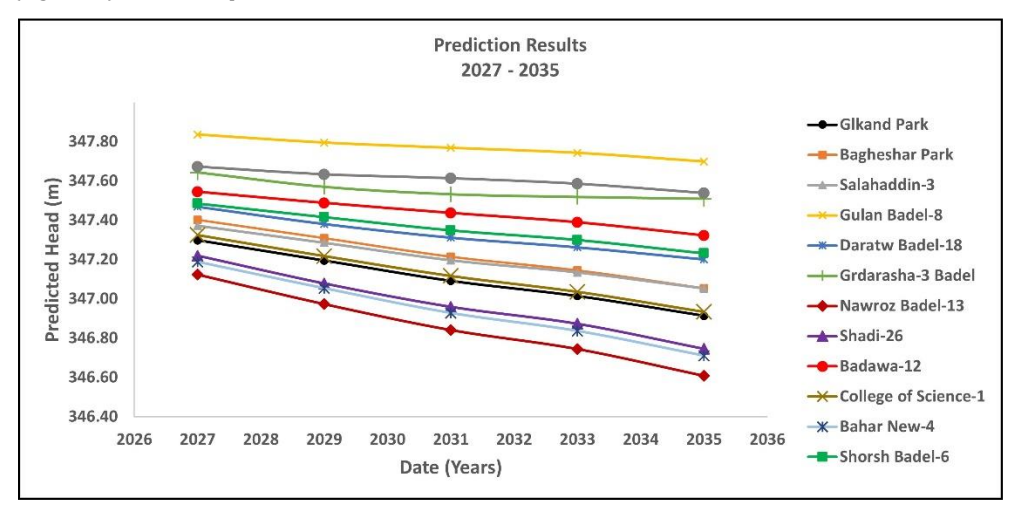


Figure 11: Prediction graphs for the Monitoring Wells

3.4 Statistical Analysis of Prediction Results

This section shows what the statistical analysis has found regarding the reliability and significance of the estimates for steady-state groundwater levels. The purpose of the analysis is to observe the changes in trends over the period being predicted. All the monitoring wells display declining levels, suggesting that in the future, the water levels in the ground could

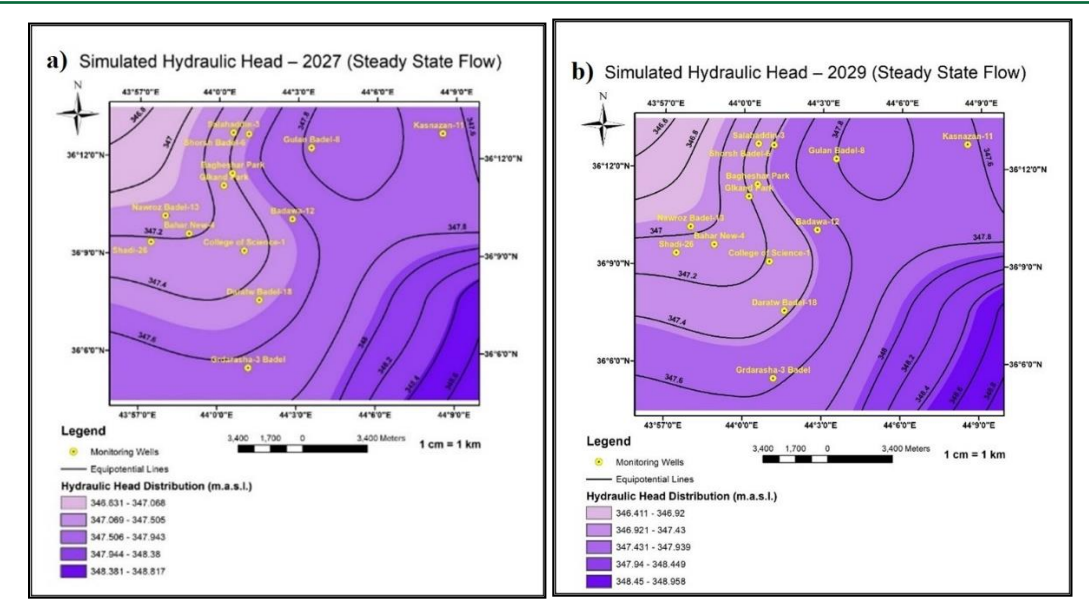
drop under the scenarios tested. The high R^2 values (from 0.827 to 0.972) indicate that the forthcoming trends of the model are a clear match for many wells. It demonstrates why knowing future trends is important for successful groundwater management. The findings for each monitoring well such as the Kendall's tau, p-values, Sen's slope and R^2 , are shown in Table (6) below.

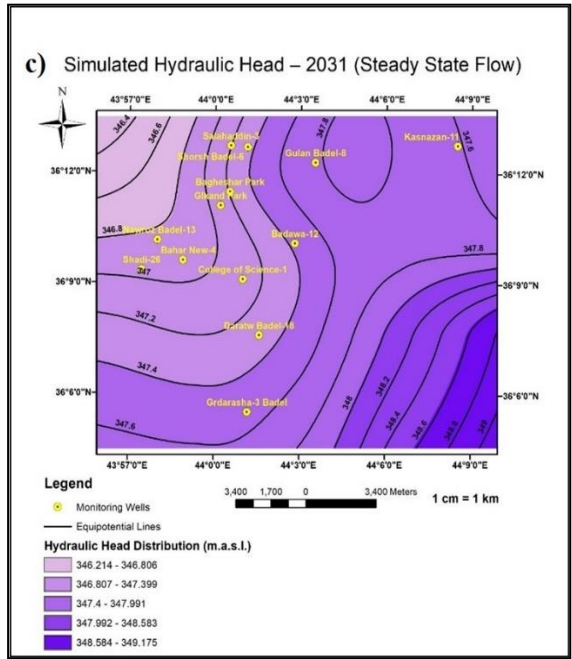
	Table 6: Statistical Analysis of Prediction Results								
#	Well Name	Kendall's tau	p-value	Sen's slope	R ²				
1	Badawa-12	-1.000	0.027	-0.027	0.961				
2	Bahar New-4	-1.000	0.027	-0.059	0.958				
3	Bagheshar Park	-1.000	0.027	-0.043	0.857				
4	College of Science-1	-1.000	0.027	-0.049	0.972				
5	Daratw Badel-18	-1.000	0.027	-0.032	0.955				
6	Glkand Park	-1.000	0.027	-0.048	0.959				
7	Grdarasha-3 Badel	-1.000	0.027	-0.015	0.827				
8	Gulan Badel-8	-1.000	0.027	-0.016	0.067				
9	Kasnazan-11	-1.000	0.027	-0.015	0.930				
10	Nawroz Badel-13	-1.000	0.027	-0.064	0.957				
11	Salahaddin-3	-1.000	0.027	-0.040	0.958				
12	Shadi-26	-1.000	0.027	-0.058	0.955				
13	Shorsh Badel-6	-1.000	0.027	-0.031	0.958				

3.5 Spatial Analysis of Prediction Results

This section presents spatial analysis of the estimated groundwater level for the years 2027, 2029, 2031, 2031 and 2035, as illustrated in figures (12 and 13). The analysis sheds light on spatial distribution and variation in the groundwater level in the field of study using continuous lines under steady state flow conditions. During the prediction period, the groundwater level was approximately 345.89 to 349.53 meters above sea level. The model constantly reveals a spatial shield pattern spread from

the southeast to the north -west, indicating localized changes in hydraulic conductivity caused by variable pump speed, with a slight change in the density of equipped lines. In all the analyzed years, the approximate current shows strong adaptation with surveillance sites, which confirms the model's ability to simulate the hygienic behavior of the aquifer system hygienic behavior correctly. This broad spatial assessment provides valuable insight into environmental law and effects of human activities over the dynamics of the groundwater flow over time.





 $\textbf{Figure 12:} \ Equipotential \ maps \ of \ predicted \ years \ (2027-2031) \ (ArcMap\ 10.8$

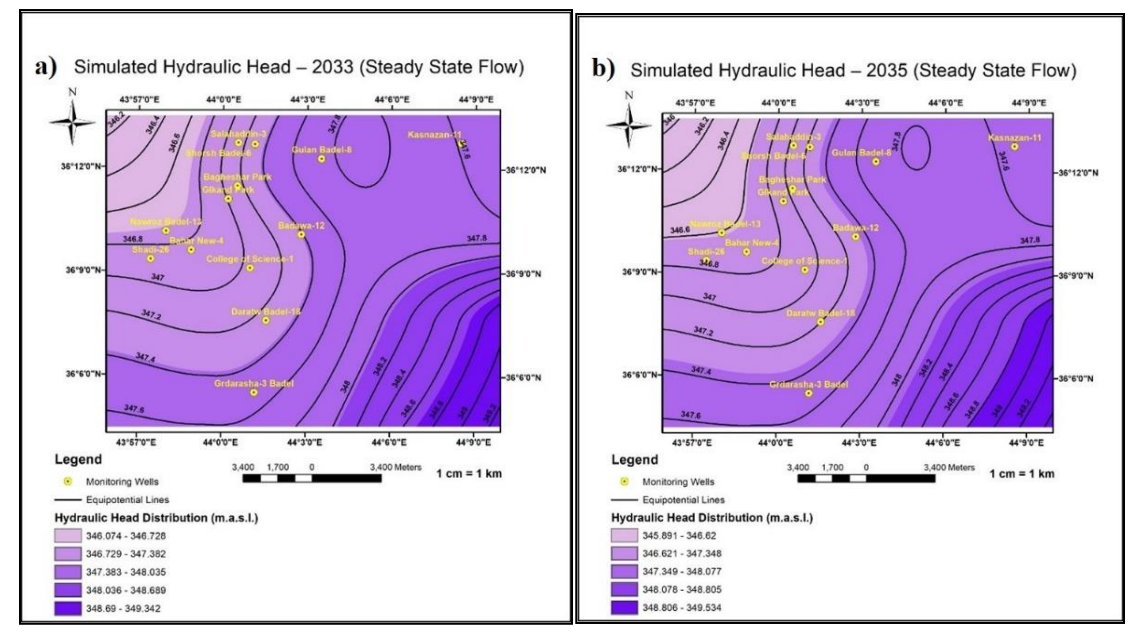


Figure 13: Equipotential maps of predicted years (2023 and 2035) (ArcMap 10.8)

4. CONCLUSIONS

This study presents a fully three-dimensional numerical groundwater flow model of the Erbil Basin, a novel advancement in the conceptualization of the hydrogeological setup of the area. Using long-term monitoring data from 2000 through 2024 and by the power of GMS 10.8.6 and spatial analysis using ArcMap 10.8, the research gives fundamental knowledge of groundwater flow under the steady-state condition.

The outcomes of the study of model calibration and validation show high accuracy with Nash-Sutcliffe Efficiency (NSE) ranging up to 0.962 %, thereby confirming the excellence of the model in modeling groundwater levels. Temporal trends reveal sustained decreasing trends of groundwater heads within the basin, mainly due to increased water demand. The variation of precipitation patterns is also influencing it. 2025–2035 predictive simulations indicate continued declining trends in groundwater levels, primarily evident in the south and southwest parts of the basin, to uncover potential limits to future water resource sustainability.

Spatial distribution of equipotential surfaces illustrates a general direction of flow from southeast to northwest with evident hydrogeological heterogeneities due to soil composition and hydraulic conductivity. These observations emphasize the necessity for continuous monitoring of groundwater levels and the necessity to densify the monitoring network in order to obtain an improved coverage of spatial and temporal variability.

Based on these results, this study recommends targeted management intervention, including leading artificial recharging projects in the most affected areas, increasing water harvesting techniques and integrating calibrated numerical models as a decision support tool for permanent groundwater management. In addition, it is necessary to add future climate studies with groundwater modeling that it is necessary to improve future to specify abilities under changed environmental conditions.

The developed model serves as a reliable framework for scenario analysis and strategic planning, thereby supporting efforts to balance water supply demands with aquifer conservation and environmental protection in the Erbil Basin.

ACKNOWLEDGMENTS

This research is part of a Master's thesis focused on the Erbil groundwater basin, covering the period from 2000 to the end of 2024, with predictions extending to 2035. The author sincerely thanks the College of Engineering at the University of Mosul, particularly the Department of Dams and Water Resources, for their continuous support throughout this study. Gratitude is also extended to the Erbil Groundwater Directorate in Erbil City, Kurdistan Region of Iraq, for their cooperation and for providing essential groundwater data. The author would also like to express appreciation to the reviewers and editorial team of the journal for their valuable time and consideration.

REFERENCES

- Abraham, B., and Ledolter, J., 2009. Statistical methods for forecasting. John Wiley and Sons.
- Akram, S., and Ann, Q. U., 2015. Newton raphson method. International Journal of Scientific and Engineering Research, 6(7), Pp. 1748-1752.
- Al-Areedhi, H., and Khayyun, T. S., 2019. Modelling of Groundwater Flow for the Iraqi Aquifers. PhD. University of Technology.
- Ali, S. S., and Salley, S. K. R., 2013. Numerical groundwater flow modeling for the intwrgranular aquifer in sarsian sub-basin, Dokan lake, Iraqi kurdistan region. Journal of Zankoy Sulaimani-Part A, 15(1), Pp. 125-141. https://doi.org/10.17656/jzs.10238.
- ALKnoo, A., 2022. Quantitative Characteristics of Groundwater and its Distribution in Tal-Afar Region-Iraq. Al-Rafidain Engineering Journal, 27(2), Pp. 156-165. https://doi.org/10.33899/rengj.2022.131941.1137.
- Al-Muqdadi, S. W., 2012. Groundwater investigation and modelingwestern desert of Iraq.
- Al-Taiee, T. M., and Hasan, A. A., 2006. Simulation and prediction of groundwater paths and flow vectors at Mosul city. Al-Rafidain Engineering Journal, 14(4), Pp. 73-81. https://doi.org/10.33899/rengj.2006.45362.
- Anderson, M. P., Woessner, W. W., and Hunt, R. J., 2015. Applied groundwater modeling: simulation of flow and advective transport. Academic press.

- Bayat, M., Eslamian, S., Shams, G., and Hajiannia, A., 2020. Groundwater level prediction through GMS software-case study of Karvan area, Iran. Quaestiones Geographicae, 39(3), Pp. 139-145. https://doi.org/10.2478/quageo-2020-0028.
- Douglas, E., Vogel, R., and Kroll, C., 2000. Trends in floods and low flows in the United States: impact of spatial correlation. Journal of hydrology, 240(1-2), Pp. 90-105. https://doi.org/10.1016/S0022-1694(00)00336-X.
- FAO., 2014. FAO Statistical Yearbook 2013, World Food and Agriculture (Food and Agriculture Organization of the United Nations, Rome, pp. 289, Issue. http://www.fao.org/docrep/018/i3107e/i3107e00.htm.
- Faqe, H., and Hashemi, S., 2015. Impact of urban growth on groundwater levels using remote sensing-case study: Erbil City, Kurdistan Region of Iraq. Nat. Sci. Res, 5, Pp. 72-84.
- Fetter, C. W., and Kreamer, D., 2021. Applied hydrogeology. Waveland Press.
- Freeze, R. A., and Cherry, J. A., 1979. Groundwater prentice-hall. Englewood Cliffs, NJ, 176, Pp. 161-177.
- Gordon, S., 2006. The normal distribution. Sydney: Mathematics Learning Centre, University of Sydney.
- Harbaugh, A. W., 2005. MODFLOW-2005, the US Geological Survey modular ground-water model: the ground-water flow process (Vol. 6). US Department of the Interior, US Geological Survey Reston, VA, USA.
- Hassan, I., 1998. Urban hydrology of Erbil city Region. PhD thesis, University of Baghdad, Baghdad.
- Hawez, D. M., Mizzouri, N. S., Aziz, S. Q., Mustafa, J. S., and Manguri, S. B. H., 2020. Groundwater characteristics assessment in Kurdistan region provinces-Iraq: A review. Journal of Duhok University, 23(2), Pp. 546-583. https://doi.org/10.26682/csjuod.2020.23.2.45.
- Hirsch, R. M., and Slack, J. R., 1984. A nonparametric trend test for seasonal data with serial dependence. Water resources research, 20(6), Pp. 727-732. https://doi.org/10.1029/WR020i006p00727.
- Ismael, S. O., and Aziz, S. Q., 2024. Population Forecasting Till 2050 Using Various Methods and Water Supply Strategy for Erbil City. Polytechnic Journal, 14(1), 6. https://doi.org/10.59341/2707-7799.1803.
- Jwan, S. M., Salah, F. S. A., and Shuokr, Q. A., 2021. Assessment of sustainability and management for groundwater source in Erbil city. Recycling and Sustainable Development, 14(1), Pp. 41-50. https://doi.org/10.5937/ror2101041M.
- K. Yenigu"n MSc, P., V. Gu"mu" s, MSc and H. Bulut MSc, PhD., 2008. Trends in streamflow of the Euphrates basin, Turkey [Water Management 161]. ICE Institution of Civil Engineers(WM4), Pages 189–198. https://doi.org/10.1680/wama.2008.161.4.189.
- Kareem, H., 2018. Study of water resources by using 3d groundwater modelling in Al-Najaf Region, Iraq Cardiff University].
- Khayyat, H. A. K. A., Sharif, A. J. M., and Crespi, M., 2019. Assessing the impacts of climate change on natural resources in Erbil area, the Iraqi Kurdistan using geo-information and Landsat data. In Environmental remote sensing and GIS in Iraq (pp. 463-498). Springer. https://doi.org/10.1007/978-3-030-21344-2_19.
- Kumar, C., 2012. Groundwater modelling software-capabilities and limitations. IOSR Journal of Environmental Science, Toxicology and Food Technology, 1(2), Pp. 46-57.
- Lerner, D. N., 2002. Identifying and quantifying urban recharge: a review. Hydrogeology Journal, 10, Pp. 143-152. https://doi.org/10.1007/s10040-001-0177-1.
- Margat, J., and Van der Gun, J., 2013. Groundwater around the world: a geographic synopsis. Crc Press.
- Merz, S. K., 2012. Australian groundwater modelling guidelines. Waterlines report series(82).
- Montgomery, D. C., Peck, E. A., and Vining, G. G., 2021. Introduction to linear regression analysis. John Wiley and Sons.
- Moriasi, D. N., Arnold, J. G., Van Liew, M. W., Bingner, R. L., Harmel, R. D., and Veith, T. L., 2007. Model evaluation guidelines for systematic

- quantification of accuracy in watershed simulations. Transactions of the ASABE, 50(3), Pp. 885-900. https://doi.org/10.13031/2013.23153.
- Mustafa, J. S., and Mawlood, D. K., 2024. Research Paper Developing threedimensional groundwater flow modeling for the Erbil Basin using Groundwater Modeling System (GMS). Journal of Groundwater Science and Engineering, 12(178), Pp. 189. https://doi.org/10.26599/JGSE.2024.9280014.
- Nanekely, M., Scholz, M., and Aziz, S. Q., 2017. Towards sustainable management of groundwater: A case study of semi-arid area, Iraqi Kurdistan region. European Water, 57, Pp. 451-457.
- Nash, J. E., and Sutcliffe, J. V., 1970. River flow forecasting through conceptual models part I—A discussion of principles. Journal of hydrology, 10(3), Pp. 282-290. https://doi.org/10.1016/0022-1694(70)90255-6.
- Niswonger, R. G., Panday, S., and Ibaraki, M., 2011. MODFLOW-NWT, a Newton formulation for MODFLOW-2005. US Geological Survey Techniques and Methods, 6(A37), 44. https://doi.org/10.5066/F7XP7317.
- Panahi, M., Misagi, F., and Asgari, P., 2018. Simulation and estimate groundwater level fluctuations using GMS (Zanjan plain). Environmental Sciences, 16(1), Pp. 1-14.
- Qarani, A. S., and Sabah, M. J., 2022. Sustainability of water supply management for Erbil City in the context of sustainable development agenda. Recycling and Sustainable Development, 15(1), Pp. 1-7. https://doi.org/10.5937/ror2201001A.
- Schweizer, B., 2015. Darcy's law and groundwater flow modelling. https://doi.org/10.14760/SNAP-2015-007-EN.
- Seeyan, S., 2020. Groundwater Flow Modeling for Qushtapa Plain Unconfined Aquifer in Southern Erbil Basin, Kurdistan Region, Iraq. Journal of Geoscience and Environment Protection, 8(03), Pp. 116. https://doi.org/10.4236/gep.2020.83009.
- Sen, P. K., 1968. Estimates of the regression coefficient based on Kendall's tau. Journal of the American statistical association, 63(324), Pp. 1379-1389. https://doi.org/10.1080/01621459.1968.10480934.
- Shekhmamundy, I. H., and Surdashy, A. M., 2022. Geomorphological analysis and distribution of landform of Erbil Masterplan Layout. The Iraqi Geological Journal, Pp. 197-211. https://doi.org/10.46717/igj.55.2F.14ms-2022-12-29.

- Singh, A., 2014. Groundwater resources management through the applications of simulation modeling: A review. Science of the total environment, 499, Pp. 414-423. https://doi.org/10.1016/j.scitotenv.2014.05.048.
- Tabari, H., Marofi, S., Aeini, A., Talaee, P. H., and Mohammadi, K., 2011. Trend analysis of reference evapotranspiration in the western half of Iran. Agricultural and forest meteorology, 151(2), Pp. 128-136. https://doi.org/10.1016/j.agrformet.2010.09.009.
- Tabari, H., Taye, M. T., and Willems, P., 2015. Statistical assessment of precipitation trends in the upper Blue Nile River basin. Stochastic environmental research and risk assessment, 29, Pp. 1751-1761. https://doi.org/10.1007/s00477-015-1046-0.
- UnitedNations., 2022. World Population Prospects 2022, Revision Population Database. Available at: https://population.un.org/wpp/ [Online]. [Accessed 25th December, 2023].
- Wang, X., Sun, Y., Xu, Z., Zheng, J., and Zhang, C., 2020. Feasibility prediction analysis of groundwater reservoir construction based on GMS and Monte Carlo analyses: A case study from the Dadougou Coal Mine, Shanxi Province, China. Arabian journal of geosciences, 13, Pp. 1-11. https://doi.org/10.1007/s12517-019-4978-8.
- Willmott, C. J., and Matsuura, K., 2005. Advantages of the mean absolute error (MAE) over the root mean square error (RMSE) in assessing average model performance. Climate research, 30(1), Pp. 79-82. https://doi.org/10.3354/cr030079.
- Yashooa, N. K., and Mawlood, D. K., 2023. Modeling contamination transport (nitrate) in Central Basin Erbil, Kurdistan region, Iraq with support of MODFLOW software. The Iraqi Geological Journal, Pp. 234-246. https://doi.org/10.46717/igj.56.1E.18ms-2023-5-28.
- Yeh, W. W., 2015. Optimization methods for groundwater modeling and management. Hydrogeology Journal, 23(6), Pp. 1051. https://doi.org/10.1007/s10040-015-1260-3.
- Zhao, X., Wang, D., Xu, H., Ding, Z., Shi, Y., Lu, Z., and Cheng, Z., 2021. Simulation and prediction of groundwater pollution based on GMS: a case study in Beijing, China. IOP Conference Series: Earth and Environmental Science. https://doi.org/10.1088/1755-1315/826/1/012014.
- Zhou, Y., and Li, W., 2011. A review of regional groundwater flow modeling. Geoscience frontiers, 2(2), Pp. 205-214. https://doi.org/10.1016/j.gsf.2011.03.003.

